Relativistic Effects in the Electromagnetic Current at GeV Energies

S. Jeschonnek and T. W. Donnelly

Center for Theoretical Physics, Laboratory for Nuclear Science and Dept. of Physics,

Massachusetts Institute of Technology, Cambridge, MA 02139, U.S.A.

(February 9, 2008)

Abstract

We employ a recent approach to the non-relativistic reduction of the electromagnetic current operator in calculations of electronuclear reactions. In contrast to the traditional scheme, where approximations are made for the transferred momentum, transferred energy and initial momentum of the struck nucleon in obtaining an on-shell inspired form for the current, we treat the problem exactly for the transferred energy and transferred momentum. We calculate response functions for the reaction $^2H(e, e'p)n$ at CEBAF (TJNAF) energies and find large relativistic corrections. We also show that in Plane Wave Impulse Approximation, it is always possible to use the full operator, and we present a comparison of such a limiting case with the results incorporating relativistic effects to the first order in the initial momentum of the struck nucleon.

25.30.Fj, 25.10+s

Typeset using REVTeX

I. INTRODUCTION

At present, there exists a broad experimental program of electron scattering studies at TJNAF, MAMI, Bates, and NIKHEF aimed at understanding the short range structure of nuclei and the properties of nucleons in the nuclear medium. In the theoretical calculation of these processes, one typically performs a non-relativistic reduction of the relativistic electromagnetic current operator, as the nuclear wave function is usually given in a non-relativistic framework. Traditionally, certain assumptions have been made for the non-relativistic reduction: the momentum $\vec{q}$ transferred from the electron to the nucleus is regarded as being smaller than the nucleon mass m_N, and the transferred energy ω and the initial momentum $\vec{p}$ of the nucleon are in turn assumed to be smaller than the transferred momentum, namely,

$$
\begin{aligned}
|\vec{q}| &< m_N \\
\omega \approx \frac{\vec{q}^2}{2m_N} &\ll m_N \\
|\vec{p}| &\ll m_N \,.
\end{aligned}
\tag{1}
$$

These approximations often cannot be justified for present day experiments, since the transferred energies and momenta may be in the GeV region and thus are comparable with or even bigger than the nucleon mass. This applies especially to TJNAF with its 4 GeV electron beam.

In the past, there have been several attempts to improve on the reduction by expanding in powers of q/m_N [1,2], but for a situation where also the transferred energies and not only the transferred momenta attain values comparable to the nucleon mass, these approaches are insufficient. Such a situation occurs and is indeed a common one, for instance, in near quasielastic kinematics. There also exist other expansion schemes [3].

In this paper, we focus on the problem of an improved treatment of the non-relativistic reduction of the electromagnetic current operator. We do not discuss here, however, the general problem of off-shell prescriptions for the current. Instead, since we treat the non-relativistic reduction in a nuclear framework, we adopt the popular ansatz of using the on-

shell form for the current and employ this form with bound and scattering wave functions for the nucleons in the nucleus. In so-doing this, we are, of course, using yet another off-shell prescription, since only with plane waves will the current matrix elements be taken strictly on-shell. The goal of the paper is to explore specific classes of non-relativistic approximations within the context of this particular ansatz, identified in this work as the "on-shell form" of the off-shell current.

Some aspects of the formalism presented in this paper have been used in other recent publications [4–6], although several approximations invoked in those studies have not been checked explicitly before using a realistic nuclear model. In this paper, we point out how to check the quality of these approximations and we present a comparison between the exact results (i.e. exact within the context of the model; see below for details) and the approximated results employing a realistic nuclear model. The calculations shown in this paper have been carried out for the reactions $^2H(e, e'p)n$ and $^2\vec{H}(\vec{e}, e'p)n$ at CEBAF energies, which are interesting in their own right.

This paper is organized as follows: First, we discuss the new approach for the single-nucleon current that treats the problem exactly for the transferred energy and transferred momentum. The approach employs the on-shell form for use in off-shell calculations. In particular, the current is expanded in powers of the initial nucleon momentum. We show that for the special case of Plane Wave Impulse Approximation and exclusive $(e, e'N)$ reactions, we can always employ the full form of the current operator. This allows us to check the quality of the expansion in powers of the initial nucleon momentum. Then we compare results which have been obtained using the non-relativistic reduction and the improved current operator, and discuss the role of the new contributions arising from the relativistic corrections.

II. THE CURRENT OPERATOR

We start our discussion with the single-nucleon on-shell electromagnetic current operator and its non-relativistic reduction. Afterwards, we discuss how the current is applied in the nucleus. Throughout this paper, we use the conventions of Bjorken and Drell [7] and base our notation on the abbreviated treatment presented in [4].

It is useful to rewrite the single-nucleon current,

$$J^\mu(P\Lambda; P'\Lambda') = \bar{u}(P'\Lambda')\left[F_1\gamma^\mu + \frac{i}{2m_N}F_2\sigma^{\mu\nu}Q_\nu\right]u(P\Lambda), \tag{2}$$

in a form that is more suitable for application to nuclear problems. The 4-momentum of the incident nucleon is $P^\mu = (E, \vec{p})$, the 4-momentum of the outgoing nucleon is $P'^\mu = (E', \vec{p}')$, and the transferred 4-momentum is $Q^\mu = P'^\mu - P^\mu$. The spin projections for incoming and outgoing nucleons are labeled Λ and Λ', respectively.

It is convenient to introduce dimensionless variables at this point:

$$\lambda \equiv \omega/2m_N$$
$$\vec{\kappa} \equiv \vec{q}/2m_N$$
$$\tau \equiv \kappa^2 - \lambda^2 \tag{3}$$
$$\vec{\eta} \equiv \vec{p}/m_N$$
$$\varepsilon \equiv E/m_N = \sqrt{1 + \eta^2}.$$

For the outgoing nucleon, $\vec{\eta}\,'$ and $\epsilon\,'$ are defined correspondingly. Of course, these latter quantities can be eliminated through 4-momentum conservation.

The Dirac and Pauli form factors are functions only of the 4-momentum transfer, $F_{1,2} = F_{1,2}(\tau)$, and in the following we use the Sachs form factors $G_E(\tau) = F_1(\tau) - \tau F_2(\tau)$ and $G_M(\tau) = F_1(\tau) + F_2(\tau)$.

Also, it is useful to introduce the angle θ between $\vec{\kappa}$ and $\vec{\eta}$, which allows us to obtain the following relations between the kinematic variables:

$$\kappa\eta\cos\theta = \lambda\varepsilon - \tau$$

$$\tau\left(\varepsilon + \lambda\right)^2 = \kappa^2\left[1 + \tau + \delta^2\right], \tag{4}$$

where δ is defined as $\delta \equiv \eta\sin\theta$. For later use we also define:

$$\mu_1 \equiv \frac{\kappa\sqrt{1+\tau}}{\sqrt{\tau}\left(\varepsilon + \lambda\right)} = \frac{1}{\sqrt{1 + \frac{\delta^2}{1+\tau}}} \tag{5}$$

$$\mu_2 \equiv \frac{2\kappa\sqrt{1+\tau}}{\sqrt{\tau}\left(1 + \tau + \varepsilon + \lambda\right)} = \frac{2\mu_1}{1 + \frac{\sqrt{\tau(1+\tau)}}{\kappa}\mu_1}. \tag{6}$$

It is our aim to obtain expressions for the single-nucleon electromagnetic current operators $\bar{J}^\mu(P; P')$ that occur inside the two component spin-$\frac{1}{2}$ spinors, *viz.*

$$J^\mu(P\Lambda; P'\Lambda') \equiv \chi_{\Lambda'}^\dagger \bar{J}^\mu(P; P')\chi_\Lambda. \tag{7}$$

The bar over the current distinguishes an operator from its spin matrix elements. Writing these in the following way with an overall factor f_0 removed for convenience (note that J^μ in Eq. (7) is a four-vector, whereas V^μ in Eq.(8) is not, although also labeled with the Lorentz index μ),

$$\bar{J}^\mu \equiv f_0 V^\mu \tag{8}$$

$$f_0 \equiv \frac{1}{\mu_1\sqrt{1 + \frac{\tau}{4(1+\tau)}\mu_2^2\delta^2}}, \tag{9}$$

the electromagnetic current operator may then be rewritten in terms of the kinematical variables introduced previously:

$$V^0 = \xi_0 + i\xi_0'\left(\vec{\kappa}\times\vec{\eta}\right)\cdot\vec{\sigma} \tag{10}$$

$$V^3 = (\lambda/\kappa)\,V^0 \tag{11}$$

$$\vec{v}^\perp = \xi_1\left[\vec{\eta} - \left(\frac{\vec{\kappa}\cdot\vec{\eta}}{\kappa^2}\right)\vec{\kappa}\right] - i\left\{\xi_1'\left(\vec{\kappa}\times\vec{\sigma}\right)\right. \tag{12}$$

$$\left. +\xi_2'\left(\vec{\kappa}\cdot\vec{\sigma}\right)\left(\vec{\kappa}\times\vec{\eta}\right) + \xi_3'\left[(\vec{\kappa}\times\vec{\eta})\cdot\vec{\sigma}\right]\left[\vec{\eta} - \left(\frac{\vec{\kappa}\cdot\vec{\eta}}{\kappa^2}\right)\vec{\kappa}\right]\right\},$$

where the coefficients ξ_i (no spin dependence) and ξ_i' (spin dependence) are given by:

$$\xi_0 = \frac{\kappa}{\sqrt{\tau}} \left[G_E + \frac{\mu_1 \mu_2}{2(1+\tau)} \delta^2 \tau G_M \right]$$

$$\xi_0' = \frac{1}{\sqrt{1+\tau}} \left[\mu_1 G_M - \frac{1}{2} \mu_2 G_E \right]$$

$$\xi_1 = \frac{1}{\sqrt{1+\tau}} \left[\mu_1 G_E + \frac{1}{2} \mu_2 \tau G_M \right]$$

$$\xi_1' = \frac{\sqrt{\tau}}{\kappa} \left(1 - \frac{\mu_1 \mu_2}{2(1+\tau)} \delta^2 \right) G_M$$

$$\xi_2' = \frac{\lambda \sqrt{\tau}}{2\kappa^3} \mu_1 \mu_2 G_M$$

$$\xi_3' = \frac{\sqrt{\tau}}{2\kappa(1+\tau)} \mu_1 \mu_2 \left[G_E - G_M \right]. \tag{13}$$

These are exact expressions for the on-shell electromagnetic current operator, also given in [4]. So far, Eq. (2) has only been rewritten. The conservation of the current is obvious from Eq. (11).

Later on, we will refer to the operator associated with ξ_o as zeroth-order charge operator, where the zeroth-order indicates that the operator, in this case the identity, is of zeroth order in η. Correspondingly, we call the term containing the ξ_o' first-order spin-orbit operator, the term containing ξ_1 first-order convection current, the term containing ξ_1' zeroth-order magnetization current, the term containing ξ_2' first-order convective spin-orbit term, and the term containing ξ_3' second-order convective spin-orbit term. Note that all coefficients ξ_i and ξ_i' contain terms that are either of zeroth or first order in η.

Compared with the fully non-relativistic reduction discussed below (compare Eqs. (27)), there are several new types of operators in Eqs. (10-12), and the operators which are also present for the non-relativistic reduction, namely the zeroth-order charge operator, the zeroth-order magnetization current and the first-order convection current, are multiplied with new factors. For the charge, we now have an additional contribution, which is traditionally called the "spin-orbit" part of the charge. It is also present in the q/m_N expansion schemes. In the transverse part of the current, there are two new operators with different spin structures (the first-order and second-order convective spin-orbit terms).

Eqs. (10) and (12), which are coordinate free, can also be rewritten using a coordinate

system with unit vectors $\vec{u}_3 \equiv \vec{\kappa}/\kappa$, $\vec{u}_2 \equiv (\vec{\kappa} \times \vec{\eta})/\kappa\eta \sin\theta$ and $\vec{u}_1 \equiv \vec{u}_2 \times \vec{u}_3$ to obtain

$$V^0 = \nu_0 + i\nu'_0\sigma^2 \tag{14}$$

$$\vec{v}^\perp = \nu_1\vec{u}_1 + i\left[\nu'_1\sigma^2\vec{u}_1 - \left(\nu'_2\sigma^1 + \nu''_2\sigma^3\right)\vec{u}_2\right], \tag{15}$$

with

$$
\begin{aligned}
\nu_0 &= \frac{\kappa}{\sqrt{\tau}}\left[G_E + \frac{\mu_1\mu_2}{2(1+\tau)}\delta^2\tau G_M\right] = \xi_0 \\
\nu'_0 &= \frac{\kappa}{\sqrt{1+\tau}}\left[\mu_1 G_M - \frac{1}{2}\mu_2 G_E\right]\delta = \kappa\delta\xi'_0 \\
\nu_1 &= \frac{1}{\sqrt{1+\tau}}\left[\mu_1 G_E + \frac{1}{2}\mu_2\tau G_M\right]\delta = \delta\xi_1 \\
\nu'_1 &= \sqrt{\tau}\left(G_M - \frac{\mu_1\mu_2}{2(1+\tau)}\delta^2 G_E\right) = \kappa\xi'_1 - \kappa\delta^2\xi'_3 \\
\nu'_2 &= \sqrt{\tau}\left(1 - \frac{\mu_1\mu_2}{2(1+\tau)}\delta^2\right)G_M = \kappa\xi'_1 \\
\nu''_2 &= = \frac{1}{2}\left(\frac{\lambda}{\kappa}\right)\sqrt{\tau}\mu_1\mu_2\delta G_M = \kappa^2\delta\xi'_2.
\end{aligned}
\tag{16}
$$

In addition to expressing the current operator with respect to the coordinate system with unit vectors $\vec{u}_1, \vec{u}_2, \vec{u}_3$, the terms in Eqs. (14),(15) have also been reordered according to which kind of Pauli matrix they contain, so that it is easy to see which terms can interfere. One can read off immediately the orders of the terms that contribute to the cross section for electron nucleon scattering. Additionally, here it is easy to see which terms do not flip the spin (those involving either no Pauli matrix or σ^3, namely, ν_o, ν_1, and ν''_2) and which do (those involving $\sigma^{1,2}$, and hence $\sigma^\pm$, namely, ν'_o, ν'_1, and ν'_2).

It is instructive to evaluate the spin matrix elements of the operator given in Eqs. (14) and (15) and from these to obtain the unpolarized single-nucleon responses (see also [8]). For example, the purely longitudinal "L" response involves non-spin-flip and spin-flip matrix elements of V^o squared and added incoherently (in the unpolarized responses, the two contributions cannot interfere):

$$f_0^2\left[\nu_0^2 + \nu'^2_0\right] = \frac{1}{1+\tau}\left\{(\varepsilon + \lambda)^2 G_E^2 + \kappa^2\delta^2 G_M^2\right\}$$

7

$$= \frac{\kappa^2}{\tau} \left\{ G_E^2 + \delta^2 W_2 \right\} , \tag{17}$$

$$\tag{18}$$

where $W_1 \equiv \tau G_M^2$ and $W_2 \equiv \frac{1}{1+\tau} [G_E^2 + \tau G_M^2]$. Similarly, the purely transverse parts of the current yield

$$f_0^2 \left[\nu_1^2 + \nu_1'^2 \right] = \frac{1}{\kappa^2} \frac{1}{1+\tau} \left\{ (\varepsilon + \lambda)^2 \tau^2 G_M^2 + \kappa^2 \delta^2 G_E^2 \right\}$$

$$= W_1 + \delta^2 W_2 \tag{19}$$

$$f_0^2 \left[\nu_2'^2 + \nu_2''^2 \right] = \tau G_M^2 = W_1 , \tag{20}$$

and from this one can see that the unpolarized "T" and "TT" responses (involving the sum and minus the difference of Eqs.(19-20), respectively) are $2W_1 + \delta^2 W_2$ and $-\delta^2 W_2$, respectively. Finally, the unpolarized "TL" response is

$$f_0^2 \left[\nu_o \nu_1 + \nu_o' \nu_1' \right] = \frac{\kappa}{\sqrt{\tau}} \sqrt{1 + \tau + \delta^2} \, \delta W_2 . \tag{21}$$

Note that in Eqs. (17-21) the form factors G_E and G_M enter only in linear combinations of G_E^2 and G_M^2. Terms of the type $G_E G_M$ do not occur, as expected.

When used in PWIA for the unpolarized cross section (including the special case of the relativistic Fermi gas model [9]) these constitute the on-shell forms for the single-nucleon electromagnetic response functions to be employed in concert with the nuclear spectral function. They bear a strong resemblance to the popular off-shell prescriptions that are widely used in treatments of $(e, e'N)$ reactions [10–12] and, in fact, at least in reasonably "safe" situations such as nearly quasifree kinematics yield results that do not differ appreciably from those of the latter. Of course, our ultimate goal is to provide current operators and their matrix elements taken with interacting initial *and* final state wave functions, in which case Eqs.(17-21) do not hold and, of course, the cross section does not factorize into single-nucleon responses multiplied by a spectral function.

In electronuclear reactions, one usually assumes that the electron emits one photon which interacts with one of the nucleons in the nucleus. Nucleons in the nucleus are bound and

therefore off-shell; they do not fulfill the same energy-momentum relations as free nucleons. Currently, there exists no microscopic description of this off-shell behavior that can be applied for a wide range of kinematic conditions — there are only ad hoc prescriptions, which lead to vastly differing results for certain kinematics [10–12].

In this paper, we want to concentrate on particular classes of non-relativistic approximations for the current, and therefore restrict our attention to the popular ansatz of applying the electromagnetic current in its on-shell form. In subsequent work we intend to widen the scope to include other approaches to more general off-shell behaviour.

When calculating matrix elements for the single-nucleon case, the initial and final states are plane waves, and therefore eigenfunctions of the operator $\vec{\eta}$. In the nuclear case, the initial and final states are single-particle wave functions for nucleons in the nucleus. The coordinate space operator corresponding to $\vec{\eta}$ is then $-i\vec{\nabla}/m_N$. Unlike the plane waves in the case of the free nucleon, the single-particle wave functions are not eigenfunctions of $\vec{\eta}$ or $\vec{\nabla}$, and this leads to a technical problem, as the operator $\vec{\eta}$ appears several times in the denominators of the ξ's in Eqs. (13) and the ν's in Eqs. (16). Therefore, we have to Taylor-expand the expressions for the current in powers of $\vec{\eta}$. Importantly, however, we never make expansions in κ or λ (and therefore τ), as discussed below.

Equations (16) have been cast in forms well suited for this task. We present the results to first order in η. From Eqs. (5) and (9) one finds that $\mu_1 = 1 + \mathcal{O}(\eta^2)$ and $f_0 = 1 + \mathcal{O}(\eta^2)$, whereas one sees that $\mu_2 = 1 + \frac{1}{2}\sqrt{\frac{\tau}{1+\tau}}\eta\cos\theta + \mathcal{O}(\eta^2)$ by using Eqs. (4–6). We then have

$$
\begin{aligned}
\nu_0 &= \frac{\kappa}{\sqrt{\tau}}G_E + \mathcal{O}(\eta^2) \\
\nu_0' &= \frac{\kappa}{\sqrt{1+\tau}}\left[G_M - \frac{1}{2}G_E\right]\eta\sin\theta + \mathcal{O}(\eta^2) \\
\nu_1 &= \frac{1}{\sqrt{1+\tau}}\left[G_E + \frac{1}{2}\tau G_M\right]\eta\sin\theta + \mathcal{O}(\eta^2) \\
\nu_1' &= \sqrt{\tau}G_M + \mathcal{O}(\eta^2) \\
\nu_2' &= \sqrt{\tau}G_M + \mathcal{O}(\eta^2) \\
\nu_2'' &= \frac{1}{2}\left(\frac{\lambda}{\kappa}\right)\sqrt{\tau}G_M\eta\sin\theta + \mathcal{O}(\eta^2),
\end{aligned}
\tag{22}
$$

9

leading to the following results for the electromagnetic current operators to linear order in η:

$$\bar{J}^0 = \frac{\kappa}{\sqrt{\tau}}G_E + \frac{i}{\sqrt{1+\tau}}\left[G_M - \frac{1}{2}G_E\right](\vec{\kappa}\times\vec{\eta})\cdot\vec{\sigma} + \mathcal{O}(\eta^2) \tag{23}$$

$$\bar{J}^3 = (\lambda/\kappa)\,\bar{J}^0 \tag{24}$$

$$\vec{\bar{J}}^\perp = -\frac{\sqrt{\tau}}{\kappa}\left\{iG_M\left([\vec{\kappa}\times\vec{\sigma}] + \frac{1}{2}\left(\frac{\lambda}{\kappa}\right)\frac{1}{\kappa}(\vec{\kappa}\cdot\vec{\sigma})(\vec{\kappa}\times\vec{\eta})\right)\right.$$
$$\left. - \left(G_E + \frac{1}{2}\tau G_M\right)\left[\vec{\eta} - \left(\frac{\vec{\kappa}\cdot\vec{\eta}}{\kappa^2}\right)\vec{\kappa}\right]\right\} + \mathcal{O}(\eta^2), \tag{25}$$

employing Eqs. (10–12) and noting from Eq. (4) that $\kappa = \sqrt{\tau(1+\tau)} + \tau\eta\cos\theta + \mathcal{O}(\eta^2)$. Of course, when computing matrix elements of these operators and then forming bilinear combinations of the results to obtain the electromagnetic observables, terms of order η^2 must be neglected if the operators themselves have been expanded only to order η, since other terms will enter from considering the neglected $\mathcal{O}(\eta^2)$ contributions in Eqs. (23–25).

As can be seen from Eqs. (22–24), at linear order in η we retain the spin-orbit part of the charge and one of the relativistic corrections to the transverse current that appeared in Eq. (12), the first order convective spin-orbit term.

The important point in our approach is that we have expanded only in η, not in the transferred momentum κ or the transferred energy λ. The momentum of the initial nucleon will be relatively low in most cases — the dimensionless Fermi momentum $\eta_F = p_F/m_N$ typically ranges from about 0.06 for deuterium to about 0.28 for heavy nuclei. However, there is a lot of interest in the investigation of the short–range properties of the nuclear wave functions which are reflected in the behavior at large momentum, and for those cases it is necessary to establish how good the approximation in η is and where it does not work.

In the next section, we will discuss the relativistic corrections to the current for the special case of a deuterium target. The deuteron's Fermi momentum of 55 MeV/c = 0.28 fm^{-1}, which corresponds to $\eta_F \approx 0.06$, is considerably smaller than the Fermi momenta of heavier nuclei. For many applications, the initial momenta involved are below the Fermi momentum, as this part of the wave function leads to large and therefore experimentally

more accessible cross sections. Note that the Fermi momentum itself is not a scale in the expansion in η, so that when we consider heavier nuclei, the convergence at the respective higher Fermi momentum will be worse than the convergence at the deuteron's smaller Fermi momentum. For this reason, we have extended our analysis of electron scattering from the deuteron in the next section to rather high missing momenta in order to draw conclusions about the convergence of the expansion in η also for the region $\eta > \eta_F^{deuteron}$ which is accessible experimentally for heavier nuclei due to their larger Fermi momenta.

Of course, for the high momentum components of the wave function, off-shell effects are expected also to be important and for a complete understanding of the problem have to be considered in addition to the relativistic corrections discussed here.

We illustrate the importance of retaining the exact expressions for κ, λ and $\sqrt{\tau}$ with a few numbers: for a momentum transfer $q = 2m_N$, i.e. $\kappa = 1$, the transferred energy under quasielastic conditions is $\omega \approx 1.2$ GeV corresponding to $\lambda \approx 0.6$ and $\tau \approx 0.6$. This leads to an extra factor $\kappa/\sqrt{\tau} \approx 1.3$ which appears in the current matrix element, and which may enter squared in the calculated observable, therefore leading to a 60% increase in that observable. Even for moderate momentum transfers, e.g. $q = m_N$, and thus $\kappa = 0.5$, the transferred energy is $\omega \approx 400$ MeV, i.e. $\lambda \approx 0.2$ and $\tau \approx 0.2$ and an extra factor $\kappa/\sqrt{\tau} \approx 1.1$, which still gives rise to a 20% increase. Apart from the factor $\kappa/\sqrt{\tau}$ which originates from the product of the upper components and the inverse factor $\sqrt{\tau}/\kappa$ which stems from the product of upper and lower components of the Dirac spinors, there also appear certain combinations of form factors in typical observables, namely, one often finds G_E^2 together with $(\sqrt{\tau}\,G_M)^2$. The latter term would be neglected in a scheme that retains only terms of leading order in $\sqrt{\tau}$, but in fact, for example, for protons assuming dipole parameterizations for the form factors those two terms become equal for $\tau \approx 0.13$, which corresponds to $|Q^2| \approx (0.98$ GeV/c $)^2$. The importance of the relativistic corrections will become even clearer in the following section discussing the results for the reactions $^2H(e,e'p)n$ and $^2\vec{H}(\vec{e},e'p)n$.

As one can see from the expressions given above, it is actually unnecessary to make expansions in κ, λ or τ at all. If one does so in spite of this, then at intermediate momentum

11

transfers the combination $G'_M \equiv \sqrt{\tau} G_M$ should be regarded as being of leading order, and not of order $1/m_N^2$ as is often assumed. With these caveats under some circumstances Eq. (25) may be approximated by

$$\vec{J}^{\perp} \cong -\frac{\sqrt{\tau}}{\kappa} \left\{ i G_M \left[\vec{\kappa} \times \vec{\sigma} \right] - G_E \left[\vec{\eta} - \left(\frac{\vec{\kappa} \cdot \vec{\eta}}{\kappa^2} \right) \vec{\kappa} \right] \right\}. \tag{26}$$

As we will compare our results with the strict non-relativistic reduction, we quote the corresponding expressions:

$$\bar{J}^o_{nonrel} = G_E$$
$$\bar{J}^{\perp}_{nonrel} = -i G_M \left[\vec{\kappa} \times \vec{\sigma} \right] + G_E \left[\vec{\eta} - \left(\frac{\vec{\kappa} \cdot \vec{\eta}}{\kappa^2} \right) \vec{\kappa} \right]. \tag{27}$$

Note that the non-relativistic reduction contains both terms of zeroth order in η and terms of first order in η, i.e. the convection current. The strict non-relativistic reduction is therefore not the lowest-order term of an expansion in η.

In our new approach, once the on-shell form has been adopted, the only approximation made is cutting off the expansion in powers of η at a certain order. Of course, it is necessary to check how good this approximation is, e.g. if it is sufficient to use the expressions up to first order in η, which are given explicitly above, or if it is necessary to include higher orders. One possibility to check the quality of the expansion is to evaluate the second-order expressions in η and compare them with the first-order results, but as we do not know the convergence properties of the power series, this gives only limited information. It is clearly desirable to compare the first-order results with the results obtained with the full form of the operator. Due to the in general complicated form of the nuclear initial and final states, this is not possible for most cases. However, for coincidence $(e, e'N)$ reactions in Plane Wave Impulse Approximation (PWIA), it is actually possible to carry out a calculation with the full current operator. In this special case, one always has an outgoing plane wave for the knocked out nucleon in the final state, and by partially integrating the single-particle matrix elements of the current twice, the operator $\vec{\eta}^2$ — it appears only squared, never in linear or cubic form — acts on the final state and thus on its eigenfunction.

III. RESULTS

We have chosen to demonstrate the effects of the relativistic corrections to the current for the reaction $^2H(e, e'p)n$ and $^2\vec{H}(\vec{e}, e'p)n$ because of the following reasons: first, realistic wave functions are available in parameterized form for this nucleus [13,14] and second, there is a lively experimental interest in the exploration of the properties of few-body systems. Specifically, there are several experiments planned at TJNAF with deuterium targets [15]. However, the current operator discussed in the previous section can be applied to any nucleus and to any type of electronuclear reaction.

An extensive discussion of coincidence reactions in general can be found in [16]; here we only quote the basic formulae. The differential cross section is equal to

$$\left(\frac{d\sigma^5}{d\epsilon' d\Omega_e d\Omega_N}\right)_{fi}^h = \frac{m_N \, m_f \, p_N}{8\pi^3 \, m_i} \, \sigma_{Mott} \, f_{rec}^{-1}$$
$$\left[\left(v_L \mathcal{R}_{fi}^L + v_T \mathcal{R}_{fi}^T + v_{TT} \mathcal{R}_{fi}^{TT} + v_{TL} \mathcal{R}_{fi}^{TL} \right) \right.$$
$$\left. + h \left(v_{T'} \mathcal{R}_{fi}^{T'} + v_{TL'} \mathcal{R}_{fi}^{TL'} \right) \right], \tag{28}$$

where m_i, m_N and m_f are the masses of the target nucleus, the ejectile nucleon and the residual system, p_N and Ω_N are the momentum and solid angle of the ejectile, ϵ' is the energy of the detected electron and Ω_e is its solid angle. The helicity of the electron is denoted by h. The coefficients v_K are the leptonic coefficients, and the $\mathcal{R}_K$ are the response functions which are defined by

$$\mathcal{R}_{fi}^L \equiv |\rho(\vec{q})_{fi}|^2$$

$$\mathcal{R}_{fi}^T \equiv |J_+(\vec{q})_{fi}|^2 + |J_-(\vec{q})_{fi}|^2$$

$$\mathcal{R}_{fi}^{TT} \equiv 2 \, \Re \left[J_+^*(\vec{q})_{fi} \, J_-(\vec{q})_{fi} \right]$$

$$\mathcal{R}_{fi}^{TL} \equiv -2 \, \Re \left[\rho^*(\vec{q})_{fi} \left(J_+(\vec{q})_{fi} - J_-(\vec{q})_{fi} \right) \right]$$

$$\mathcal{R}_{fi}^{T'} \equiv |J_+(\vec{q})_{fi}|^2 - |J_-(\vec{q})_{fi}|^2$$

$$\mathcal{R}_{fi}^{TL'} \equiv -2 \, \Re \left[\rho^*(\vec{q})_{fi} \left(J_+(\vec{q})_{fi} + J_-(\vec{q})_{fi} \right) \right], \tag{29}$$

where the $J_\pm$ are the spherical components of the current.

For our calculations, we have chosen the following kinematic conditions: the z-axis is parallel to $\vec{q}$, the missing momentum is defined as $\vec{p}_m \equiv \vec{q} - \vec{p}_N$, so that in PWIA, the missing momentum is equal to the negative initial momentum of the struck nucleon in the nucleus, $\vec{p}_m = -\vec{p}$. We denote the angle between $\vec{p}_m$ and $\vec{q}$ by θ, and the term "parallel kinematics" indicates $\theta = 0^o$, "perpendicular kinematics" indicates $\theta = 90^o$, and "antiparallel kinematics" indicates $\theta = 180^o$. Note that both this definition of the missing momentum and the definition with the other sign are used in the literature. If not stated otherwise, we assume that the experimental conditions are such that the kinetic energy of the outgoing nucleon and the angles of the missing momentum, θ and the azimuthal angle ϕ, are fixed. If not mentioned otherwise, the kinetic energy of the outgoing proton is fixed to 1 GeV. For changing missing momentum, the transferred energy and momentum change accordingly — for the convenience of the reader, we have listed the values of the transferred energy and momentum for different kinematic conditions in Tables I and II. In antiparallel kinematics, the transferred momentum decreases with increasing missing momentum until a point is reached where the kinematical limit for the process is reached, i.e. where the transferred 4-momentum becomes timelike. This occurs at $p_m = 2.7$ fm^{-1}. For this reason, the curves showing results for antiparallel kinematics are cut off at this value. The strong increase or decrease that can be observed for some cases at this point is just an artifact: when the responses are multiplied with the corresponding leptonic coefficients, the product goes to zero.

The curves shown in this paper have been obtained using the realistic Bonn wave function [13] for the deuteron and we do not present results for other wave functions as we concentrate on the relativistic effects in the current, which are expected to be similar no matter which wave function one employs. In future work, other cases will be discussed.

A. Unpolarized Responses

In Fig. 1, we show the results for the longitudinal response $\mathcal{R}_L$ and in Fig. 2 the transverse response $\mathcal{R}_T$ calculated with the full current operator, the current operator to $\mathcal{O}(\eta)$, and the strict non-relativistic limit. In order to facilitate the comparison between the different results in all regimes of the missing momentum, we have included both linear and logarithmic plots throughout this paper. For all the different kinematics, the approximation of the electromagnetic current operator to $\mathcal{O}(\eta)$ is in good agreement with the results obtained with the full current. The two curves practically coincide up to missing momenta $p_m \approx 1.3 - 1.5 \text{ fm}^{-1}$, and the difference for higher missing momentum is small. This behavior is to be expected, as in PWIA the missing momentum coincides with the momentum of the initial nucleon inside the nucleus, which is precisely the quantity in which we have expanded the current operator. We have only expanded up to the first order of the initial momentum, and it is quite surprising that the agreement is so good up to such rather high momenta. This indicates that the expansion coefficients of the higher powers of η are rather small. In contrast to this, the results obtained within the strict non-relativistic limit disagree strongly — except for parallel kinematics — with the results that include relativistic effects. From the linear plots, it is clear that there is a significant disagreement even for the low missing momenta. This disagreement of relativistic and non-relativistic treatment of the current increases up to almost one order of magnitude for the higher p_m.

Let us examine the validity of the assumptions stated in Eq. (2) that enter the strict non-relativistic reduction. For the three different kinematics presented here, the transferred energy ω increases with increasing missing momentum (see Table I), and therefore the assumption that $\omega \ll m_N$ is never fulfilled; it actually evolves to $\omega > m_N$ for higher p_m. The initial momentum, i.e. p_m, remains smaller than the nucleon mass, but comes quite close to it. Finally, the transferred momentum q behaves differently for the different kinematic conditions (see Table II). For antiparallel kinematics, it decreases; for perpendicular kinematics, it decreases slightly; and for parallel kinematics, it increases. In all cases, how-

15

ever, it remains above the nucleon mass. For parallel kinematics, in spite of the fact that both transferred energy and transferred momentum are larger than m_N, the relation $\omega < q$ holds, which in the form of $\omega \approx q^2/2m_N$ enters the non-relativistic reduction. This is the reason for the comparatively better performance of the non-relativistic reduction in parallel kinematics.

After these general considerations, let us turn our attention to the more specific effects of the relativistic corrections on the different responses. For the longitudinal response $\mathcal{R}_L$, the relativistic corrections lead to an increase of the response function. The bulk of this effects stems from the factor $\kappa/\sqrt{\tau}$ which is contained in ξ_0 and multiplies the zeroth-order charge operator. It reaches values of more than 1.5, and it enters squared in the response. In addition, a new type of operator, the first-order spin-orbit term, appears in the relativistic treatment. This operator is already known from the q/m_N expansions, but in our treatment of the relativistic effects it has a modified factor which multiplies it. Note that in a q/m_N expansion scheme, the factor $\kappa/\sqrt{\tau}$ would be treated as 1.

For the transverse response $\mathcal{R}_T$, the relativistic corrections lead to a decrease of the response. This is due to the factor $\sqrt{\tau}/\kappa$ that multiplies the whole transverse current. The fact that here $\sqrt{\tau}/\kappa$ appears rather than its inverse as in $\mathcal{R}_L$ stems from the fact that the latter arises at leading order from upper $\times$ upper spinor components whereas here upper $\times$ lower components occur at leading order, bringing in an extra factor of τ/κ^2. The zeroth-order magnetization current is by far the largest contribution to the transverse current, and it completely dominates $\mathcal{R}_T$. The first-order convection current and the new types of operators which appear only in the relativistic treatment become important only for the interference response functions.

In order to get a different perspective, we present in Fig. 3 the longitudinal response $\mathcal{R}_L$ (left side) and the transverse response $\mathcal{R}_T$ (right side) for fixed momentum transfer $|\vec{q}| = 1.4$ GeV/c, corresponding to $\kappa = 0.75$, and fixed y, which implies a fixed energy transfer in turn. For the definition of y, see [17]. The middle panels of Fig. 3 show the responses under quasi-elastic conditions, the top panels are kinematically "below" the quasi-elastic peak, the

lower panels are "above" the quasi-elastic peak. In this choice of kinematics, the angle θ between the missing momentum and the z-axis changes with the missing momentum, as does the kinetic energy of the outgoing proton. In contrast to the previously considered kinematic setting, the value of $\kappa/\sqrt{\tau}$ does not change. Again, there is good agreement for the fully relativistic and first-order results.

The transverse response is dominated by the zeroth-order magnetization current. Therefore, the difference between the non-relativistic result and the first-order result is given by the factor $\sqrt{\tau}/\kappa$ which has the value 0.90, 0.85, and 0.74 for the top, middle, and lower panels. Obviously, the relativistic effects are largest for the largest energy transfer. The exact relativistic results tend to be larger than the first-order results at higher missing momenta because, although the coefficient ξ_1' of the zeroth-order magnetization current decreases with increasing missing momentum, the overall factor f_o, which only appears in the full calculation, increases.

In contrast to the transverse response, the longitudinal response has significant contributions from two terms: the zeroth-order charge operator and the first-order spin-orbit term. The two contributions do not interfere. The relativistic effects in the zeroth-order charge operator are similar to the effects in the zeroth-order magnetization current when one replaces the factor $\sqrt{\tau}/\kappa$ with $\kappa/\sqrt{\tau}$. The first-order spin-orbit term does not enter in the non-relativistic calculation, and its presence in the first-order results increases the difference of the non-relativistic and first-order treatment.

In Fig. 4 , we show the interference response functions $\mathcal{R}_{TT}$ and $\mathcal{R}_{TL}$. The transverse-transverse response function is negative throughout the considered range, and is very small relative to $\mathcal{R}_{L,T}$. As discussed in the previous section (see Eqs.(19-20)) this behavior is expected, since the spin-averaged unpolarized response is proportional to δ^2. As these responses both vanish in parallel and antiparallel kinematics, we present them only for perpendicular kinematics. The transverse-longitudinal response function falls between $\mathcal{R}_{L,T}$ and $\mathcal{R}_{TT}$ in magnitude, again as expected from the guidance provided by the spin-averaged unpolarized response discussed above (see Eq.(21)) where this contribution is seen to be

17

proportional to δ. Here the full results and the results to first order in the initial nucleon momentum agree extremely well up to $p_m = 4$ fm^{-1}. The non-relativistic results are considerably lower over the whole range of missing momenta, roughly by a factor 5. At first sight, this may look surprising, as one might expect that the factors which were responsible for the main difference between the relativistic and non-relativistic results for the longitudinal and the transverse responses, namely $\kappa/\sqrt{\tau}$ and $\sqrt{\tau}/\kappa$ would be multiplied yielding 1, and that therefore there would be no overall relativistic effects. However, the transverse-longitudinal response function has a different structure than $\mathcal{R}_L$ and $\mathcal{R}_T$, as seen in Eq. (29). The response $\mathcal{R}_{TL}$ consists of two different contributions: one contains the product of the first-order spin-orbit term and the zeroth-order magnetization current, the other one contains the product of the zeroth-order charge operator and the first-order convection current (see also [5,6]). The former amounts to roughly two thirds of the total response, the latter to one third. As the spin-orbit operator appears only in the relativistic treatment, it is clear that the major contribution to $\mathcal{R}_{TL}$ is completely missed in the strict non-relativistic limit. Also, the second contribution increases when the relativistic effects are taken into account: besides the two factors mentioned above which cancel each other, the factor that multiplies the first-order convection current increases from G_E to $G_E + \frac{1}{2}\tau\, G_M$, which for protons gives an extra factor of approximately $1 + 1.4\tau$, assuming dipole parameterization for the form factors. Note that those results hold under all kinematical conditions — they are not specific for perpendicular kinematics. In [18], a microscopic calculation was carried out for the $^2H(e, e'p)$ reaction at lower energies, and this calculation found large relativistic effects in $\mathcal{R}_{TL}$. As our results show, those large relativistic effects can be attributed to the current; it is not necessary to incorporate relativistic dynamics in order to see large relativistic effects (see also [19]).

As noted above, the transverse-transverse response function is the smallest of all the responses. As can be seen in Fig. 4, for this response the relative difference between the first-order and full results is the largest one we have encountered so far. This is to be expected, as the transverse-transverse response is explicitly a quantity of second order in

η (see Eqs.(19-20)), so the second-order contributions to the current, i.e. the second-order convective spin-orbit term, will contribute significantly to this response, too. Up to $p_m = 1.5$ fm^{-1}, the first-order results are slightly larger than the non-relativistic results. For $p_m > 3$ fm^{-1}, the first-order result starts to be smaller and disagrees more with the exact result, whereas the non-relativistic and exact relativistic calculations approach each other. The transverse-transverse response function is the product of two currents and because of this it has a unique structure, as seen in Eq. (29). Due to this structure, the zeroth-order magnetization current by itself cannot contribute. This fact reflects that the response is of second order — it therefore cannot have a zeroth-order contribution. As the zeroth-order magnetization current is the largest of the components of the transverse current, this explains why $\mathcal{R}_{TT}$ is so small. It also means that in the non-relativistic limit, only the first-order convection current can contribute. At first order in the expansion in η, the first-order convective spin-orbit term (see Eq. (24)), enters. This relativistic correction gives rise to a new, additive contribution to $\mathcal{R}_{TT}$. It has the opposite sign compared with the first-order convection current contribution, and although it is small, at higher p_m it is big enough to overcompensate the rise in the first-order convection current contribution due to relativistic effects. From the first order to the full current, the first-order convection current contribution rises more than the relativistic correction contribution, which in itself already amounts to an increase in $\mathcal{R}_{TT}$. However, there is still another new component of the current that arises only in the exact expression, the second-order convective spin-orbit term (see Eq. (12)). The contribution of this new operator alone is quite small, but due to the different spin structure that it has (the same as the first-order spin-orbit term in the charge operator), it can interfere with the zeroth-order magnetization current, which leads to a sizable new contribution of second order in η. This new contribution is the main reason for the discrepancy between the full result and the first-order result: one of the major contributions to the transverse-transverse response function is present only in the exact treatment of the current. In the full relativistic calculation, the second-order convective spin-orbit term also interferes with the first-order convection current and the

19

first-order convective spin-orbit term, but those contributions are much smaller than that of the interference of the second-order convective spin-orbit term with the zeroth-order magnetization current. The fact that the non-relativistic results seem to approach the exact ones for higher missing momentum is therefore mere coincidence.

In Fig. 5, we show the interference response functions $\mathcal{R}_{TT}$ and $\mathcal{R}_{TL}$ for the same kinematic conditions as used in Fig. 3. For the transverse-longitudinal response, the value of $\kappa/\sqrt{\tau}$ is not significant because of the cancellation discussed earlier, and therefore the difference between the non-relativistic and relativistic results is roughly the same for all different kinematics, in contrast to the longitudinal and transverse responses. For the transverse-transverse response, the difference between the non-relativistic and exact relativistic results also remains roughly constant under the different kinematic conditions, but the first-order results shift from the vicinity of the exact results towards the non-relativistic curve, and for the highest energy transfer, coincides more or less with the non-relativistic results. This shows that terms of second order in η play an important role here, namely the second-order convective spin-orbit term, which was discussed above.

B. Polarized Responses

After this discussion of the response functions that arise for unpolarized beam and unpolarized target nucleus, let us discuss some of the polarization observables. As the number of polarization response functions is quite high, we will just discuss two representative examples: the response $\mathcal{R}_{T'}^{M_J=1}$, which is nonzero only for a polarized target and polarized electron beam, and the response $\mathcal{R}_{TL'}^{M_J=1}$. For the discussion of those responses, we will assume that the target is completely polarized in the $M_J = 1$ state, hence the superscript $M_J = 1$. The direction of the momentum transfer serves as polarization axis.

In Fig. 6, the absolute value of the response $\mathcal{R}_{T'}^{M_J=1}$ is shown for calculations with the full current operator, the current operator to $\mathcal{O}(\eta)$, and the strict non-relativistic limit. The behavior of the different curves is very similar to the case of the transverse response function

discussed previously: For antiparallel and perpendicular kinematics, the non-relativistic result differs from the relativistic treatment considerably, especially for high p_m. For parallel kinematics, all curves are quite similar, for the reasons discussed above. The agreement between the first-order calculation and the full calculation is excellent at lower missing momenta. The largest contribution to $\mathcal{R}_{T'}^{M_J=1}$ comes from the zeroth-order magnetization current, and its behavior governs the behavior of the response. The relativistic treatment introduces the factor $\sqrt{\tau}/\kappa$, which reduces the current and the response. In the non-relativistic limit, the contribution from the first-order convection current is negligible. To first order in η, there is a very small contribution from the interference of the first-order convection current and the first-order convective spin-orbit term. In the exact calculation, there is an additional contribution from the interference between the zeroth-order magnetization current and the second-order convective spin-orbit term which appears only in the full treatment of the current operator. However, those are only small corrections to the dominant contribution of the zeroth-order magnetization current itself.

For in-plane kinematics, the $\mathcal{R}_{TL'}^{M_J=1}$ vanishes in parallel and antiparallel kinematics, so we show it only for perpendicular kinematics in Fig. 7. The most striking feature of Fig. 7 is the fact that in the non-relativistic limit, this response is negligible; the actual numbers are around 10^{-14} fm^{-3} sr^{-1}, whereas the response is quite sizable once the relativistic corrections are included. For the special case of perpendicular kinematics at the non-relativistic level, the only contribution to $\mathcal{R}_{TL'}^{M_J=1}$ contains the product of the zeroth-order charge operator and the first-order convection current. For general kinematics (see the discussion of the next figure), the product of the zeroth-order charge operator and the zeroth-order magnetization current also enters. Once the first order in η is considered, the products of the zeroth-order magnetization current and the first-order spin-orbit term of the charge operator and the product of the first-order convective spin-orbit term and the zeroth-order charge operator contribute to the response, leading to a magnitude that is comparable with the magnitude of $\mathcal{R}_{TL}$. Again, the contribution that includes the zeroth-order magnetization current is the dominant one. The second contribution has the opposite sign and its size is about 20%

to 30% of the zeroth-order magnetization current/first-order spin-orbit contribution. For first order in η, the response is negative for low p_m, it changes sign at $p_m = 1.6$ fm^{-1} and continues to be positive. The full result coincides with the first-order results up to $p_m \approx 2$ fm^{-1}, but it later changes sign again, therefore becoming quite different from the first-order result for the highest missing momenta considered here.

In Fig. 8, we show the response $\mathcal{R}_{TL'}^{M_J=1}$ for fixed q and y. Under those non-perpendicular conditions, the non-relativistic result is of comparable size to that of the relativistic result. The vanishing of the product of the zeroth-order charge operator and the zeroth-order magnetization current in perpendicular kinematics is due to the fact that it is proportional to spherical harmonics that vanish for $\theta = 90^o$. Note that the spherical harmonics would be modified (and non-zero) once a final state interaction is included. Still, the difference between non-relativistic and relativistic treatment is considerable, especially for the higher values of y and therefore of the energy transfer.

The current presented in this paper can be applied to heavy nuclei immediately, and the relativistic effects for heavy nuclei in a certain kinematical situation, i.e. for a given set of p_m, θ, and q and ω, will be similar to what has been found for the deuteron. One should keep in mind that the Fermi momentum of heavy nuclei is larger than the rather small Fermi momentum of the deuteron. Thus, even if one takes the point of view that one is interested only in the region below the Fermi momentum, where the cross section is larger and consequently easier to access experimentally than at high p_m, one will need to consider higher missing momenta for heavier nuclei where relativistic effects are expected to be larger.

IV. CONCLUSIONS

In this paper, we have investigated the relativistic effects that appear in the electromagnetic current operator. In order to perform a calculation of electronuclear reactions, we have chosen the popular off-shell prescription of using what we have called the "on-shell form of

the operator".

There are several calculations of particular electronuclear reactions for few-body targets in a microscopic fashion [18,20]. Naturally, these approaches contain relativistic treatments of the nuclear dynamics and the current. However, it is difficult to extend these approaches to higher energies — the problems start above the pion emission threshold — and they appear unlikely to be applied to heavier nuclei in the near future. The current operator discussed in this paper is not restricted by these limitations, as it can be used regardless of energy and target.

We have presented a formalism that allows one to perform the non-relativistic reduction of the free single-nucleon electromagnetic current operator without any approximation in the transferred momentum or transferred energy. Within the context of the chosen so-called on-shell form the only remaining approximation is to expand in powers of the initial momentum of the nucleon. In this paper, we have carried out a systematic investigation of the quality of this approximation by comparing the results obtained with the current to first order in η with the full results for the special case of the $(e, e'p)$ coincidence reaction in Plane Wave Impulse Approximation. This is the only case for which the exact relativistic calculation of the current can be applied to a realistic nuclear wave function. Although the assumption of PWIA at those energies is incomplete (see e.g. [21,22]), the PWIA is a valuable and reliable testing ground for the relativistic effects in the operator.

We have found very good agreement between the full relativistic treatment and the first-order results in almost all cases. In the special case of the PWIA, the quantity in which we have expanded, the momentum of the initial nucleon, coincides with the negative missing momentum. As expected, the $\mathcal{O}(\eta)$ and exact results may become somewhat different for missing momenta $p_m \approx 3$ fm $^{-1}$ and higher.

Naturally, the size of the relativistic corrections depends on the specific kinematics. The non-relativistic results are far from the full calculation and even far from the first-order results, especially for non-parallel kinematics.

Our results show that at GeV energies, it is necessary to take into account the relativistic

corrections to the electromagnetic current operator. We have also shown that it is satisfactory to include these corrections up to the first order in the initial momentum of the nucleon. The results in this paper have been obtained for the reactions $^2H(e, e'p)n$ and $^2\vec{H}(\vec{e}, e'p)n$, but the conclusions drawn here can immediately be applied to other target nuclei and, using straightforward extensions of the ideas presented, to all other electronuclear reactions.

ACKNOWLEDGMENTS

REFERENCES

[1] K. W. McVoy and L. Van Hove, *Phys. Rev.* **125** (1962) 1034.

[2] S. Boffi, C. Giusti, and F. D. Pacati, *Nucl. Phys.* **A336** (1980) 416; C. Giusti and F. D. Pacati, *Nucl. Phys.* **A336** (1980) 427.

[3] J. Adam, Jr. and H. Arenhövel, *Nucl. Phys.* **A614** (1997) 289; F. Ritz, H. Göller, T. Wilbois, and H. Arenhövel, *Phys. Rev. C* **55** (1997) 2214.

[4] J. E. Amaro, J. A. Caballero, T. W. Donnelly, A. M. Lallena, E. Moya de Guerra, and J. M. Udías, *Nucl. Phys.* **A602** (1996) 263.

[5] J. E. Amaro, J. A. Caballero, T. W. Donnelly, and E. Moya de Guerra, *Nucl. Phys.* **A611** (1996) 163.

[6] J. E. Amaro and T. W. Donnelly, MIT/CTP preprint #2600, to be published in *Ann. Phys.*

[7] J. D. Bjorken and S. D. Drell, *Relativistic Quantum Mechanics* (McGraw-Hill, New York, 1964).

[8] W. M. Alberico, T. W. Donnelly, and A. Molinari, *Nucl. Phys.* **A512** (1990) 541.

[9] R. Cenni, T. W. Donnelly, and A. Molinari, *Phys. Rev. C* **56** (1997) 276.

[10] T. de Forest Jr., *Nucl.Phys.* **A392** (1983) 232.

[11] H. W. L. Naus, S. J. Pollock, J. H. Koch, and U. Oelfke, *Nucl. Phys.* **A509** (1990) 717.

[12] J. A. Caballero, T. W. Donnelly, and G. I. Poulis, *Nucl. Phys.* **A555** (1993) 709.

[13] R. Machleidt, K. Holinde, and C. Elster, *Phys. Rep.* **149** (1987) 1.

[14] M. Lacombe, B. Loiseau, R. Mau, J. Côtè, P. Pirès, and R. Tourreil, *Phys. Lett.* **B101** (1981) 139.

[15] see e.g. P. E. Ulmer (spokesperson) CEBAF Proposal No. E-94-004; G. Petratos

(spokesperson), CEBAF Proposal No. E-91-026; E. J. Beise and S. Kox (spokespersons) CEBAF Proposal No. E-94-018; J. M. Finn, P. E. Ulmer (spokespersons) CEBAF Proposal No. E-89-028; R. J. Holt (spokesperson) CEBAF Proposal No. E-89-012.

[16] A. S. Raskin and T. W. Donnelly, *Ann. of Phys.* **191** (1989) 78.

[17] D. B. Day, J. S. McCarthy, T. W. Donnelly, and I. Sick, *Annu. Rev. Nucl. Part. Sci.* **40** (1990) 357.

[18] E. Hummel and J. A. Tjon, *Phys. Rev. C* **49** (1994) 21.

[19] G. I. Poulis and T. W. Donnelly, *Nucl. Phys.* **A577** (1994) 528.

[20] J. W. Van Orden, N. Devine, and F. Gross, *Phys. Rev. Lett.* **75** (1995) 4369.

[21] A. Bianconi, S. Jeschonnek, N. N. Nikolaev and B. G. Zakharov, *Phys. Lett.* **B343** (1995) 13.

[22] A. Bianconi, S. Jeschonnek, N. N. Nikolaev and B. G. Zakharov, *Phys. Rev. C* **53** (1996) 576.

TABLES

TABLE I.   The transferred energy ω in GeV and the dimensionless energy transfer λ for increasing missing momentum p_m. The kinetic energy of the outgoing proton is 1 GeV. The energy transfer does not depend on the angles of the missing momentum.

p_m/fm^{-1}	$\omega/$ GeV	λ
0	1.00	0.53
1	1.02	0.55
2	1.08	0.58
3	1.17	0.63

TABLE II. The transferred momentum q in GeV/c, the dimensionless momentum transfer κ, the dimensionless negative 4-momentum transfer τ, and the ratio κ / $\sqrt{\tau}$ for increasing missing momentum p_m. The kinetic energy of the outgoing proton is 1 GeV. The momentum transfer depends on the angles of the missing momentum: the top part gives the values for parallel kinematics, the middle part for perpendicular kinematics, and the lower part for antiparallel kinematics. Note that for parallel kinematics, the highest accessible missing momentum is $p_m = 2.7$ fm^{-1}.

p_m/fm^{-1}	q / GeV/c	κ	τ	$\kappa/\sqrt{\tau}$
0	1.70	0.90	0.53	1.23
1	1.89	1.01	0.72	1.19
2	2.09	1.11	0.91	1.16
3	2.29	1.22	1.10	1.16
0	1.70	0.90	0.53	1.23
1	1.68	0.90	0.51	1.26
2	1.65	0.88	0.44	1.33
3	1.59	0.85	0.33	1.48
0	1.70	0.90	0.53	1.23
1	1.50	0.80	0.34	1.37
2	1.30	0.69	0.15	1.78
3	1.10	0.59	< 0	-

FIG. 1. The longitudinal response function $\mathcal{R}_L$ is shown for parallel kinematics (a and b), perpendicular kinematics (c and d), and antiparallel kinematics (e and f). The solid line shows the response calculated with the full expression for the current operator, the dashed line is the result of the $\mathcal{O}(\eta)$ calculation and the dash-dotted line represents the result of the strict non-relativistic reduction. Note the different ranges of the missing momentum p_m for the linear plots (left) and the logarithmic plots (right).

FIG. 2. The transverse response function $\mathcal{R}_T$ is shown for parallel kinematics (a and b), perpendicular kinematics (c and d), and antiparallel kinematics (e and f). The solid line shows the response calculated with the full expression for the current operator, the dashed line is the result of the $\mathcal{O}(\eta)$ calculation and the dash-dotted line represents the result of the strict non-relativistic reduction. Note the different ranges of the missing momentum p_m for the linear plots (a,c,e) and the logarithmic plots (b,d,f).

FIG. 3. The longitudinal response function $\mathcal{R}_L$ (a,c,e) and the transverse response function $\mathcal{R}_T$ (b,d,f) are shown for fixed 3-momentum transfer $|\vec{q}|$ and different values of the y variable, which is defined as the negative minimal missing momentum (see e.g. [17]). The corresponding fixed energy transfers ω are 0.61 GeV (a and b), 0.75 GeV (c and d), and 0.94 GeV (e and f). The kinematic conditions in the middle panels correspond to quasifree conditions. Note that the angle θ varies with changing missing momentum. The solid line shows the response calculated with the full expression for the current operator, the dashed line is the result of the $\mathcal{O}(\eta)$ calculation and the dash-dotted line represents the result of the strict non-relativistic reduction.

FIG. 4. The negative transverse-transverse response function $\mathcal{R}_{TT}$ (a and b) and the transverse-longitudinal response function $\mathcal{R}_{TL}$ (c and d) are shown for perpendicular kinematics. The solid line shows the response calculated with the full expression for the current operator, the dashed line is the result of the $\mathcal{O}(\eta)$ calculation and the dash-dotted line represents the result of the strict non-relativistic reduction. Note the different ranges of the missing momentum p_m for the linear plots (a,c,e) and the logarithmic plots (b,d,f).

FIG. 5. The negative transverse-transverse response function $\mathcal{R}_{TT}$ and the transverse-longitudinal response function $\mathcal{R}_{TL}$ are shown for fixed 3-momentum transfer $|\vec{q}|$ and different values of the y variable. The corresponding fixed energy transfers ω are 0.61 GeV (a and b), 0.75 GeV (c and d), and 0.94 GeV (e and f). The kinematic conditions in the middle panels correspond to quasifree conditions. Note that the angle θ varies with changing missing momentum. The solid line shows the response calculated with the full expression for the current operator, the dashed line is the result of the $\mathcal{O}(\eta)$ calculation and the dash-dotted line represents the result of the strict non-relativistic reduction.

FIG. 6. The absolute value of the response function $\mathcal{R}_{T'}^{M_J=1}$ is shown for parallel kinematics (a and b), perpendicular kinematics (c and d), and antiparallel kinematics (e and f). The response is negative for parallel and antiparallel kinematics, for perpendicular kinematics it starts out negative and switches sign at $p_m = 1.6$ fm $^{-1}$. The solid line shows the response calculated with the full expression for the current operator, the dashed line is the result of the $\mathcal{O}(\eta)$ calculation and the dash-dotted line represents the result of the strict non-relativistic reduction. The target is assumed to be completely polarized in the $M_J = 1$ state. Note the different ranges of the missing momentum p_m for the linear plots (a,c,e) and the logarithmic plots (b,d,f).

FIG. 7. The absolute value of the response function $\mathcal{R}_{TL'}^{M_J=1}$ is shown for perpendicular kinematics. The solid line shows the response calculated with the full expression for the current operator, the dashed line is the result of the $\mathcal{O}(\eta)$ calculation and the dash-dotted line represents the result of the strict non-relativistic reduction. Both first order and exact result are negative for low p_m and change sign at $p_m = 1.6$ fm^{-1}. Whereas the first order result continues to be positive, the exact result changes sign again for $p_m = 3.8$ fm^{-1}. The target is assumed to be completely polarized in the $M_J = 1$ state. Note the different ranges of the missing momentum p_m for the linear plot (a) and the logarithmic plot (b).

FIG. 8. The absolute value of the response function $\mathcal{R}_{TL'}^{M_J=1}$ is shown for fixed 3-momentum transfer $|\vec{q}|$ and different values of the y variable. The corresponding fixed energy transfers ω are 0.61 GeV (a), 0.75 GeV (b), and 0.94 GeV (c). The kinematic conditions in the middle panels correspond to quasifree conditions. Note that the angle θ varies with changing missing momentum. The solid line shows the response calculated with the full expression for the current operator, the dashed line is the result of the $\mathcal{O}(\eta)$ calculation and the dash-dotted line represents the result of the strict non-relativistic reduction. In all cases, the response has a minus sign up to $p_m = 1.5$ fm^{-1}, and becomes and stays positive afterwards.

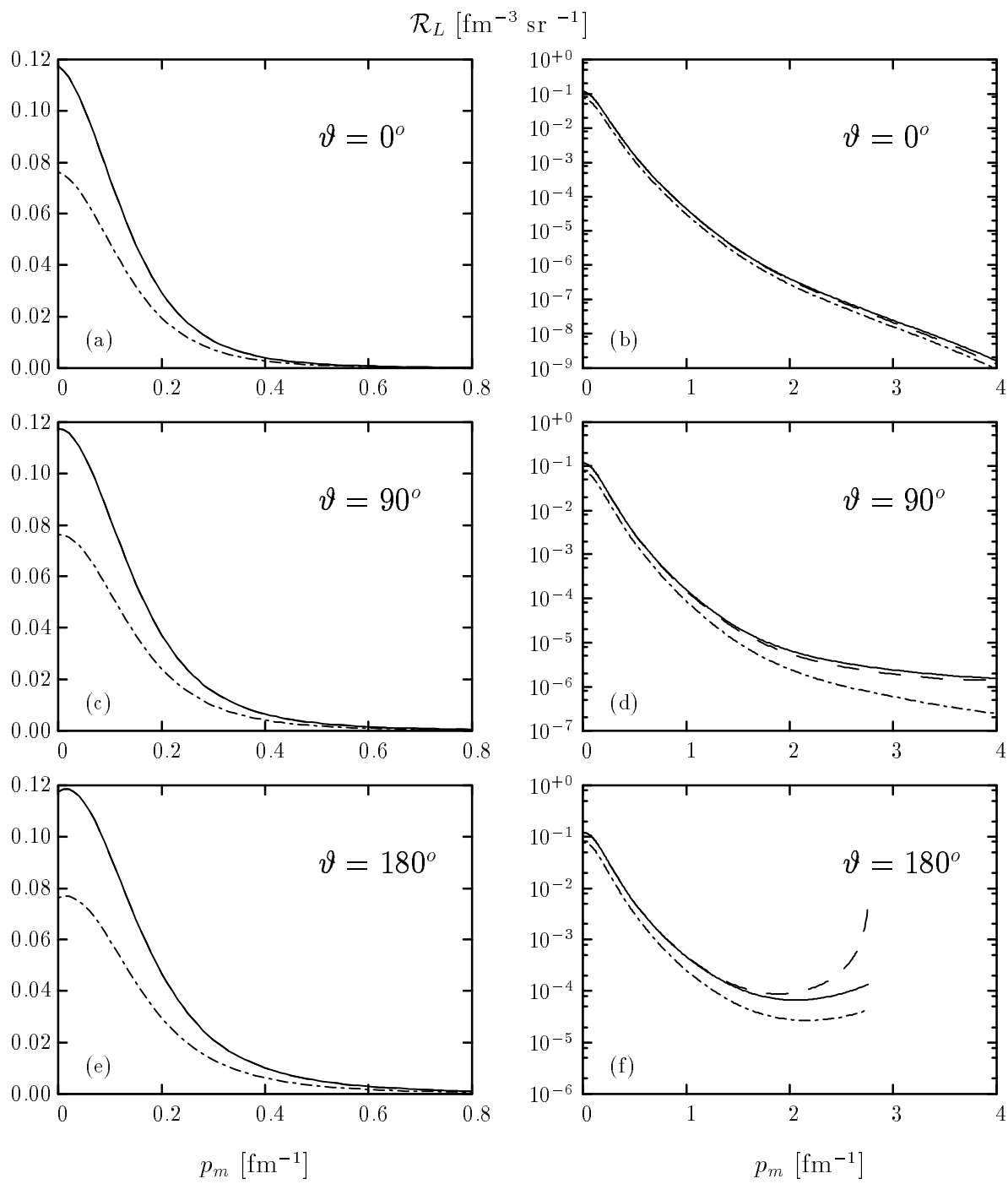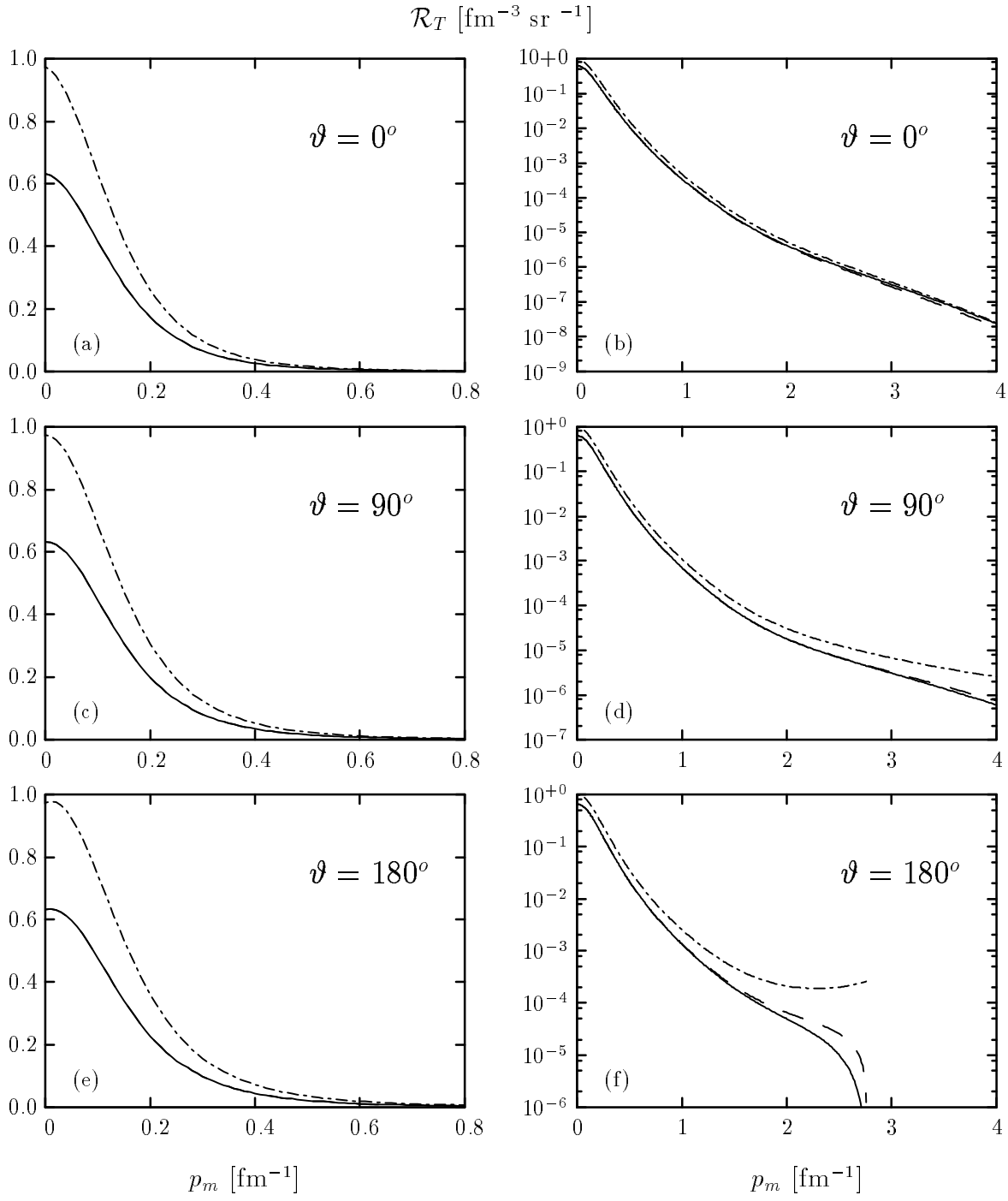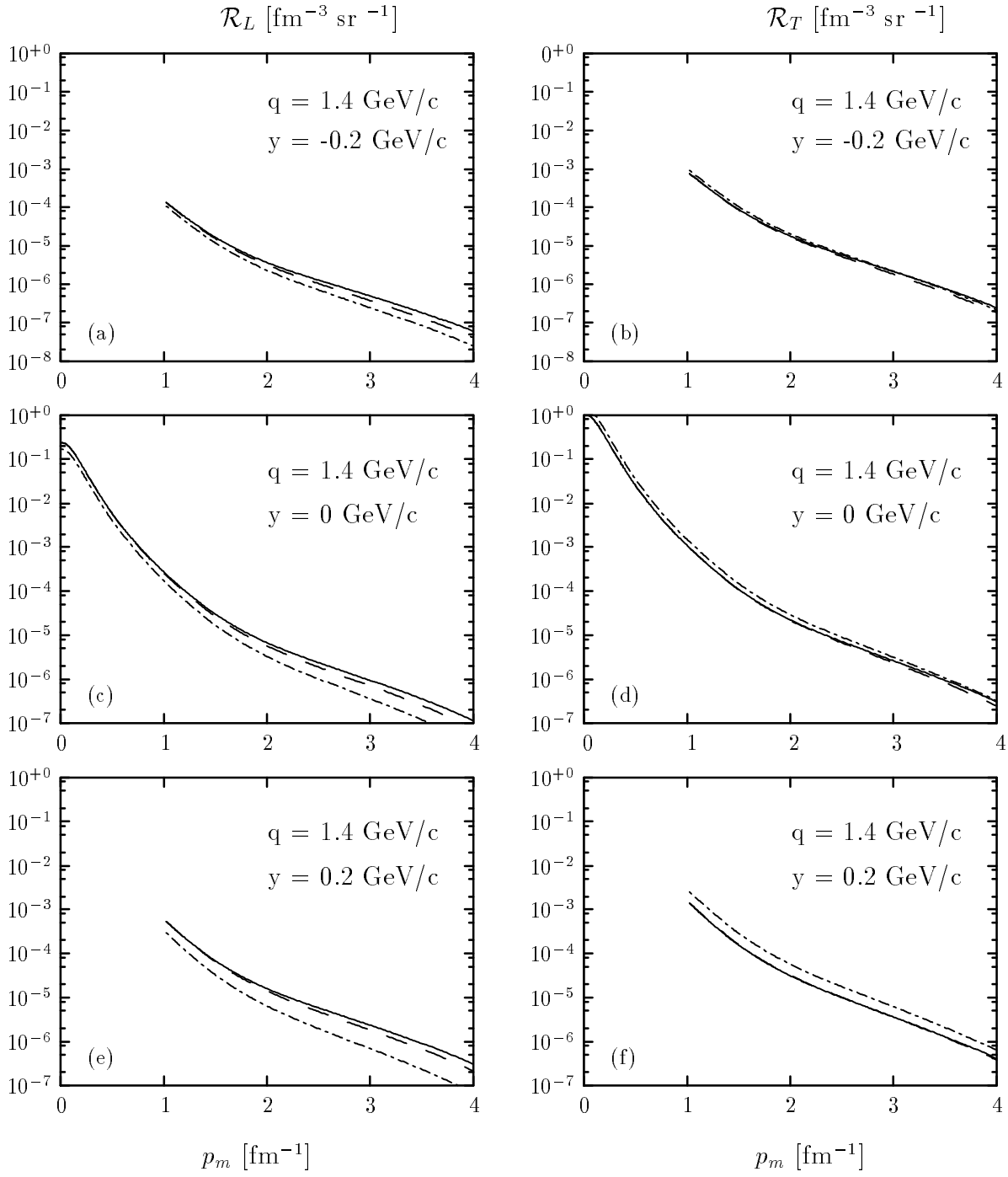$\mathcal{R}_L$ [fm^{-3} sr^{-1}]

Figure 1

$\mathcal{R}_T$ [fm^{-3} sr^{-1}]

$\vartheta = 0^o$

(a)

$\vartheta = 0^o$

(b)

$\vartheta = 90^o$

(c)

$\vartheta = 90^o$

(d)

$\vartheta = 180^o$

(e)

$\vartheta = 180^o$

(f)

p_m [fm^{-1}]

p_m [fm^{-1}]

Figure 2

Figure 3

Figure 4

$-\mathcal{R}_{TT}$ [fm^{-3} sr^{-1}] $\mathcal{R}_{TL}$ [fm^{-3} sr^{-1}]

(a) q = 1.4 GeV/c, y = -0.2 GeV/c

(b) q = 1.4 GeV/c, y = -0.2 GeV/c

(c) q = 1.4 GeV/c, y = 0 GeV/c

(d) q = 1.4 GeV/c, y = 0 GeV/c

(e) q = 1.4 GeV/c, y = 0.2 GeV/c

(f) q = 1.4 GeV/c, y = 0.2 GeV/c

p_m [fm^{-1}]

Figure 5

$|\mathcal{R}_{T'}^{M_J=1}|$ $[\text{fm}^{-3} \text{ sr}^{-1}]$

p_m $[\text{fm}^{-1}]$
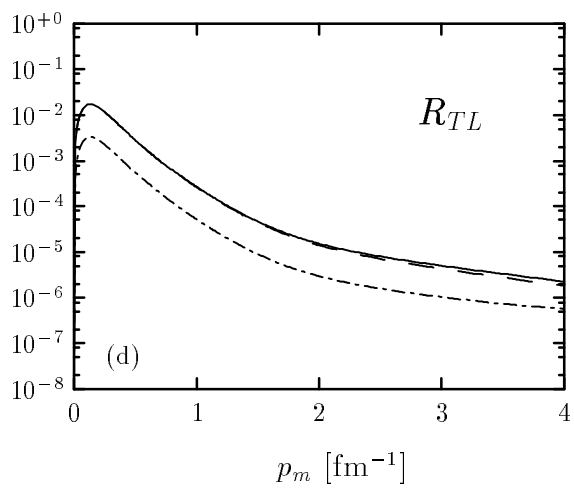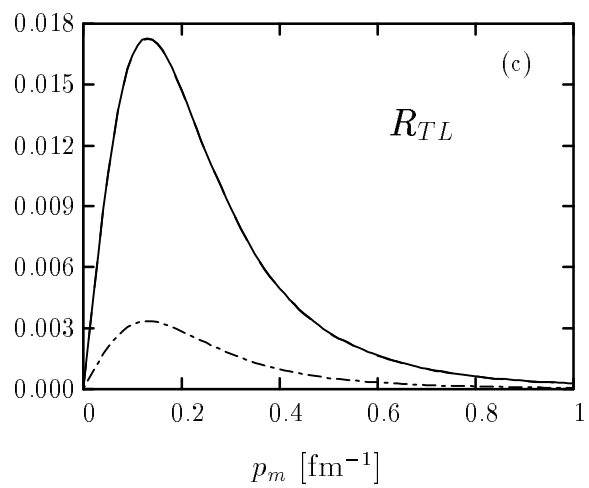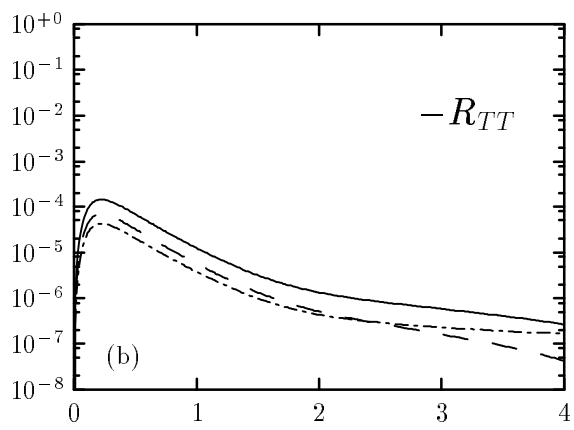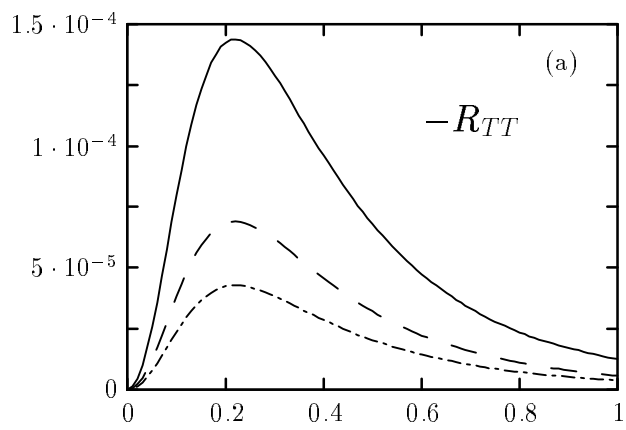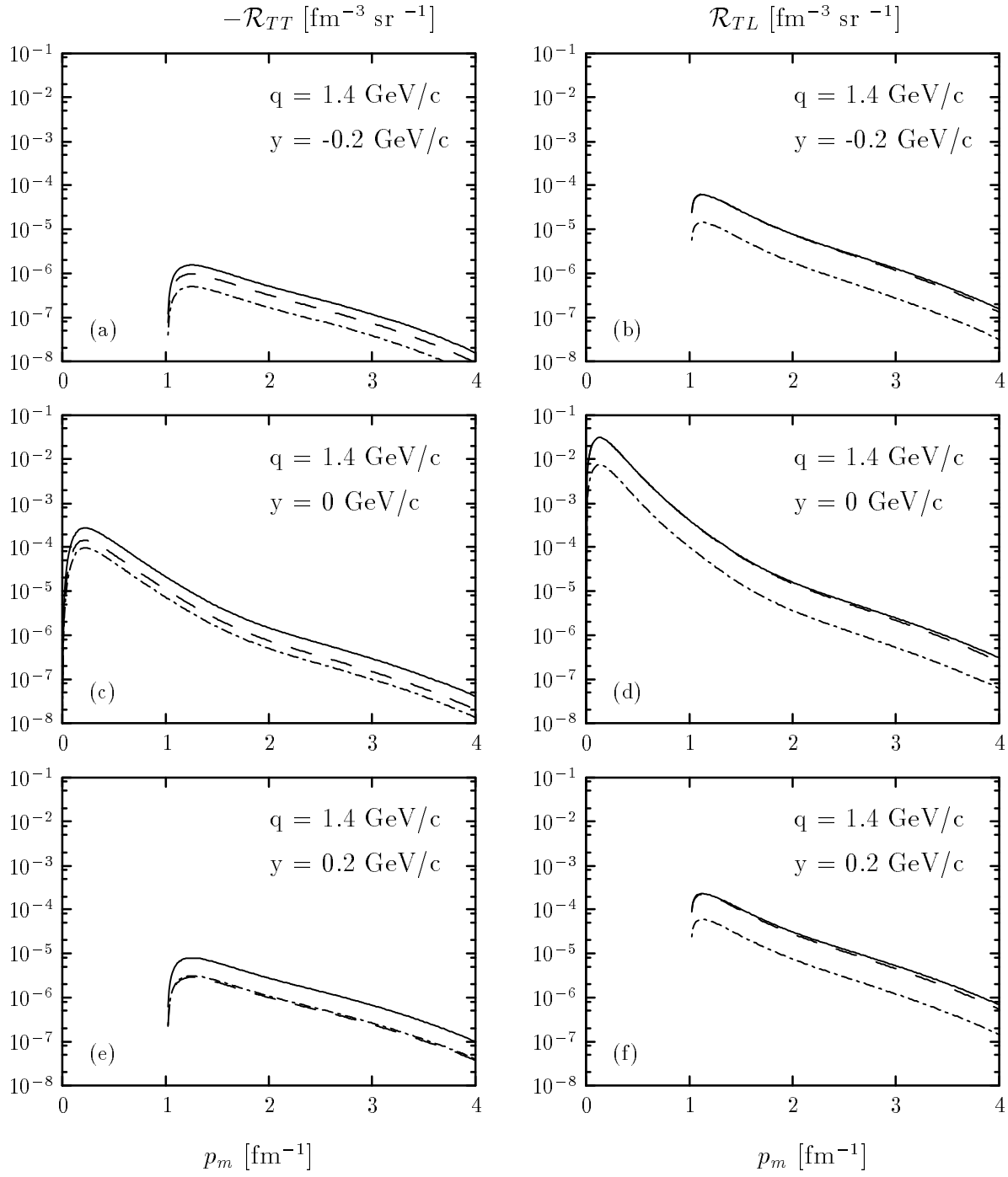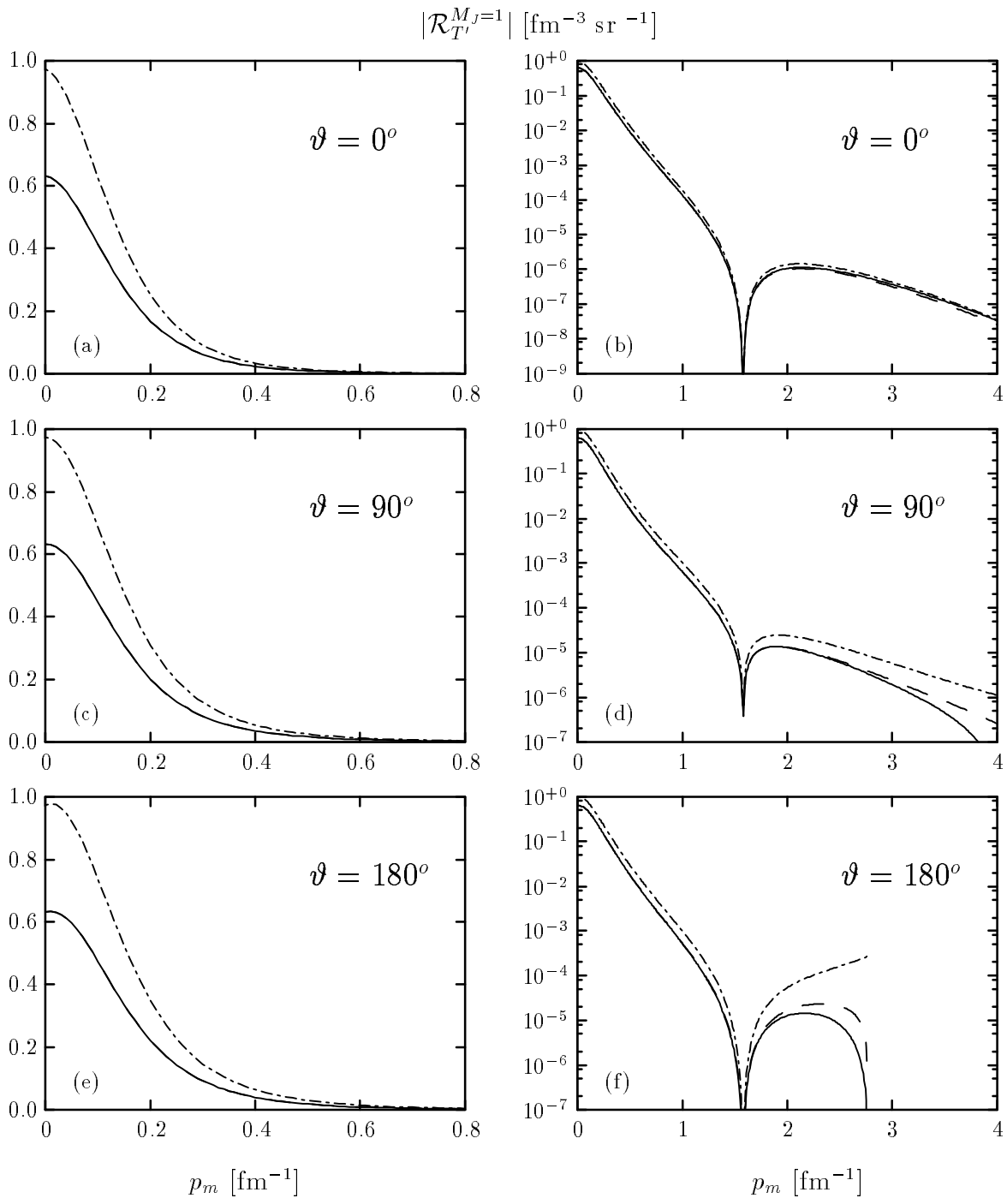
Figure 6

$$|R_{TL'}^{M_J=1}| \; [\mathrm{fm}^{-3} \; \mathrm{sr}^{-1}]$$

Figure 7

$|\mathcal{R}_{TL'}^{M_J=1}|$ [fm^{-3} sr^{-1}]

(a)

q = 1.4 GeV/c

y = -0.2 GeV/c

(b)

q = 1.4 GeV/c

y = 0 GeV/c

(c)

q = 1.4 GeV/c

y = 0.2 GeV/c

p_m [fm^{-1}]

Figure 8